NACA L-69

NATIONAL ADVISORY COMMITTEE FOR AERONAUTICS

WARTIME REPORT

ORIGINALLY ISSUED

February 1946 as
Restricted Bulletin L5K21

VARIATION OF HYDRODYNAMIC IMPACT LOADS WITH FLIGHT-PATH ANGLE FOR A PRISMATIC FLOAT AT 6° AND 9° TRIM AND A $22\frac{1}{2}°$ ANGLE OF DEAD RISE

By Sidney A. Batterson and Thelma Stewart

Langley Memorial Aeronautical Laboratory
Langley Field, Va.

NACA

WASHINGTON

NATIONAL ADVISORY COMMITTEE FOR AERONAUTICS

RESTRICTED BULLETIN

VARIATION OF HYDRODYNAMIC IMPACT LOADS WITH FLIGHT-PATH ANGLE FOR A PRISMATIC FLOAT AT 6° AND 9° TRIM AND A $22\frac{1}{2}^\circ$ ANGLE OF DEAD RISE

By Sidney A. Batterson and Thelma Stewart

SUMMARY

Tests were made in the Langley impact basin to determine the relationship between impact normal acceleration and flight-path angle for seaplanes landing in smooth water. The tests were made at both high and low forward speeds and at trims of 6° and 9°. The model had a $22\frac{1}{2}^\circ$ angle of dead rise and a gross weight of 1100 pounds. The results of the tests indicated that, over the test range of flight-path angle γ, the maximum impact normal acceleration was proportional to $\gamma^{1.54}$ for 6° trim and to $\gamma^{1.33}$ for 9° trim. At low flight-path angles the dynamic lift forces resulting from the downward deflection induced in the water impinging upon the float bottom predominated, whereas at high flight-path angles the forces resulting from the virtual mass predominated. The maximum depth of immersion and the immersion that occurred at the instant of maximum normal force showed very little effect of trim.

INTRODUCTION

Tests made in the Langley impact basin to determine the effect of flight-path angle upon impact normal acceleration for seaplanes landing in smooth water have been described in references 1 and 2. These tests were part of an investigation undertaken to determine the effect of flight-path angle upon impact accelerations throughout the range of symmetrical landings. Since the trim determines the relative effect upon the total impact load of the dynamic lift forces due to the downward deflection of the water impinging upon the float bottom and the forces resulting from the rate of change of the virtual mass, the

investigation included tests at various trims. The results presented in references 1 and 2 show the variation of impact normal acceleration with flight-path angle for trims of 3° and 12°, respectively. As a continuation of the investigation, data are presented herein to show the variation of impact normal acceleration with flight-path angle at trims of 6° and 9°. The tests were made with a model having prismatic form and a $22\frac{1}{2}^{\circ}$ angle of dead rise. The effect of weight is not included, since the total model weight was held constant throughout the tests.

SYMBOLS

V	resultant velocity of float, feet per second
V_h	horizontal velocity component of float, feet per second
V_v	vertical velocity component of float, feet per second
g	acceleration of gravity (32.2 ft/sec^2)
F_{i_w}	impact force normal to water surface, pounds
W	total model weight, pounds
$n_{i_{w_{max}}}$	maximum impact load factor $\left(\frac{F_{i_w}}{W}\right)$
τ	float trim, degrees
γ	flight-path angle, degrees $\left(\tan \gamma = \frac{V_v}{V_h}\right)$
y	vertical displacement of float, inches

EQUIPMENT AND INSTRUMENTATION

The Langley impact basin float model M-1 tested, which has a $22\frac{1}{2}^{\circ}$ angle of dead rise, was the forebody of the float described in reference 3. The lines and pertinent dimensions of this model are shown in figure 1. The gross weight of the model including the drop linkage

was 1100 pounds. The equipment and instruments used throughout the tests were, with the exception of the accelerometer, the same as those described in reference 3. An NACA air-damped accelerometer with a frequency of approximately 21 cycles per second was used to determine the impact normal acceleration.

TEST PROCEDURE

The model was tested with 0° angle of yaw at trims of 6° and 9°. The horizontal velocities for these tests ranged from approximately 45 feet per second to approximately 100 feet per second, and the vertical velocities ranged from approximately $1\frac{1}{2}$ feet per second to 12 feet per second. The range of flight-path angle was from 1° to 14°. The depth of immersion was measured at the model stern perpendicular to the level water surface. During the impact process a lift equal to the total weight of the model was exerted on the float by means of the buoyancy engine described in reference 3. All test measurements were recorded as time histories.

PRECISION

The apparatus used in the present tests yield measurements that are believed correct within the following limits:

Horizontal velocity, foot per second	±0.5
Vertical velocity, foot per second	±0.2
Vertical displacement, inch	±0.2
Acceleration, g	±0.5
Weight, pounds	±2.0

RESULTS AND DISCUSSION

For each run an accelerometer record was obtained from which the maximum load factor for each impact was derived. Since the buoyancy engine contributed a force equal to the total weight of the model, 1 g was subtracted from the values obtained from the accelerometer record to isolate the hydrodynamic force resulting from the impact.

Inasmuch as the maximum impact normal acceleration was shown in reference 3 to be proportional to the square of the resultant velocity, the hydrodynamic load factor was divided by V^2 to make it independent of velocity. The values of $n_{i_{w_{max}}}/V^2$ for both float trims of 6° and 9° are plotted in figure 2 against flight-path angle at the instant of water contact. Within the scatter of the test points appearing in this figure, the variation of $n_{i_{w_{max}}}$ with γ is a simple power function over the test range. Evaluation of the slopes of the curves in figure 2 shows that for 6° trim

$$n_{i_{w_{max}}} \propto \gamma^{1.54}$$

and for 9° trim

$$n_{i_{w_{max}}} \propto \gamma^{1.33}$$

Figure 2 indicates that at low flight-path angles the impacts for 9° trim resulted in higher loads than those for 6° trim; however, as the flight-path angle increased, the two curves tended to intersect. This condition is described in reference 4 and is attributed to the fact that at low flight-path angles the increased trim produces greater downward angle of water deflection, which results in greater impact acceleration. On the other hand, at the high flight-path angles the increase of virtual mass primarily governs the magnitude of the impact accelerations since the depth of immersion increases as the flight-path angle becomes larger. The mass effects are obviously greater in the case of the lower trim.

Maximum depth of immersion and depth of immersion at time of $n_{i_{w_{max}}}$ are plotted against flight-path angle for trim of 6° in figure 3 and for trim of 9° in figure 4. A comparison of figures 3 and 4 shows them to be nearly identical and indicates that the difference in trim had no significant effect on depth of immersion. The test range of flight-path angles was not sufficient to show the very marked effect of chine immersion upon the depth of penetration at the time of maximum force as observed

in reference 2; however, for both the 9° and 6° trims the curves exhibited reduced slopes at the higher flight-path angles.

CONCLUSIONS

Tests were made in the Langley impact basin to determine the relationship between the impact normal acceleration and flight-path angle for seaplanes landing in smooth water. The results of the tests, which were made at constant weight and model trims of 6° and 9°, lead to the following conclusions:

1. The maximum impact normal acceleration for 6° trim was proportional to $\gamma^{1.54}$ over the test range of flight-path angle γ.

2. The maximum impact normal acceleration for 9° trim was proportional to $\gamma^{1.33}$ over the test range of γ.

3. The experimental data provided a check for the previously drawn theoretical conclusion that: at low flight-path angles the lift forces resulting from the downward deflection induced in the water impinging upon the float bottom predominated, whereas at high flight-path angles the forces resulting from the virtual mass predominated.

4. The maximum depth of immersion and the immersion that occurred at the instant of maximum normal force showed very little effect of trim.

Langley Memorial Aeronautical Laboratory
National Advisory Committee for Aeronautics
Langley Field, Va.

REFERENCES

1. Batterson, Sidney A.: Variation of Hydrodynamic Impact Loads with Flight-Path Angle for a Prismatic Float at 3° Trim and with a $22\frac{1}{2}^{\circ}$ Angle of Dead Rise. NACA RB No. L5A24, 1945.

2. Batterson, Sidney A.: Variation of Hydrodynamic Impact Loads with Flight-Path Angle for a Prismatic Float at 12° Trim and with a $22\frac{1}{2}^{\circ}$ Angle of Dead Rise. NACA RB No. L5K21a, 1945.

3. Batterson, Sidney A.: The NACA Impact Basin and Water Landing Tests of a Float Model at Various Velocities and Weights. NACA ACR No. L4H15, 1944.

4. Mayo, Wilbur L.: Theoretical and Experimental Dynamic Loads for a Prismatic Float Having an Angle of Dead Rise of $22\frac{1}{2}^{\circ}$. NACA RB No. L5F15, 1945.

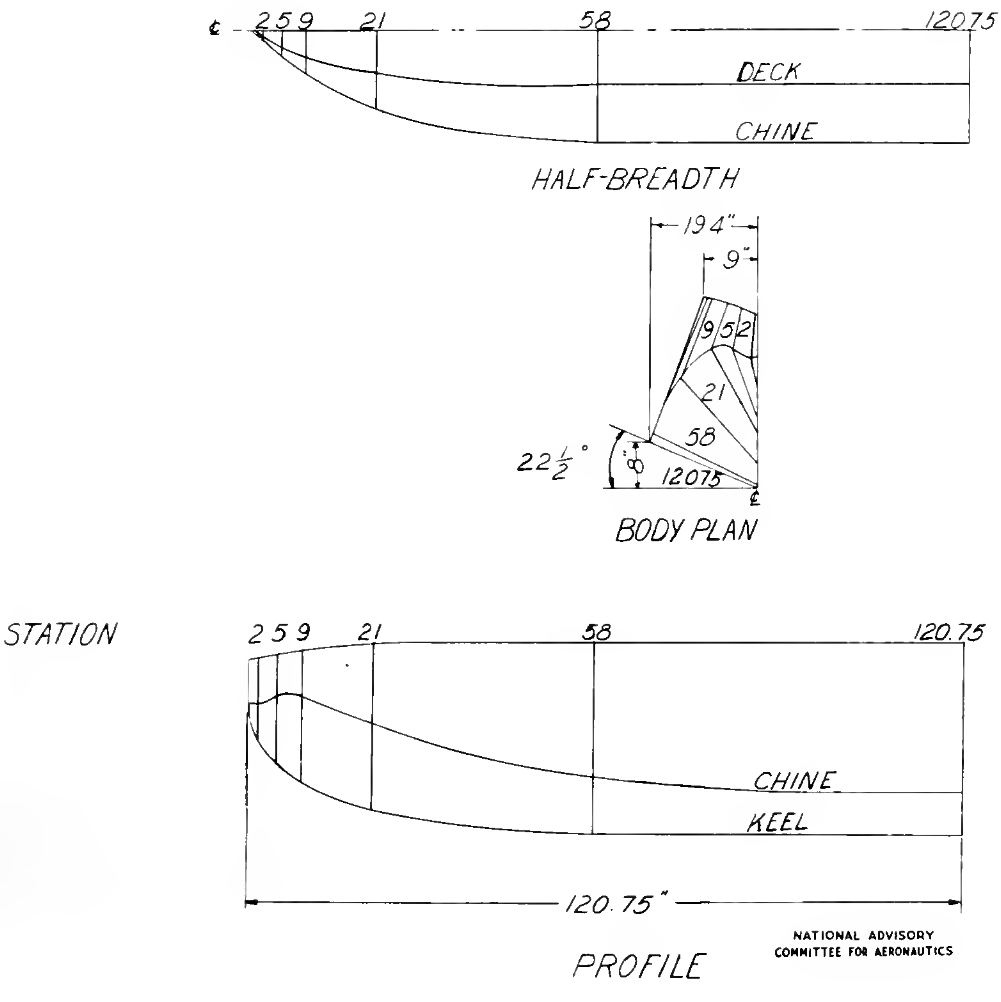

FIGURE 1.- LINES OF FLOAT MODEL M-1 TESTED IN LANGLEY IMPACT BASIN.

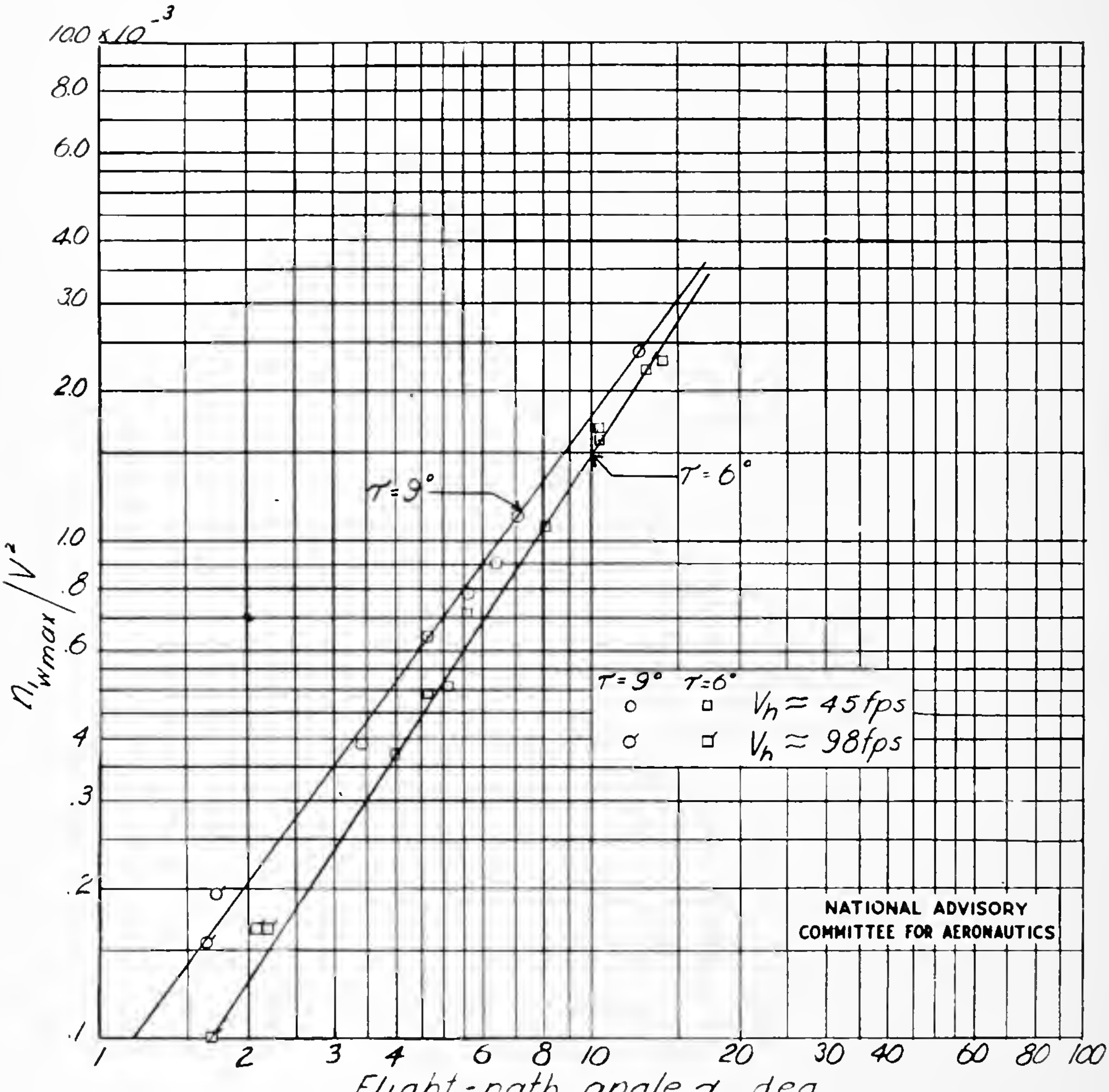

Figure 2.- Variation of parameter $n_{i_{w_{max}}}/V^2$ with flight-path angle for trims of 6° and 9°; W=1100 pounds.

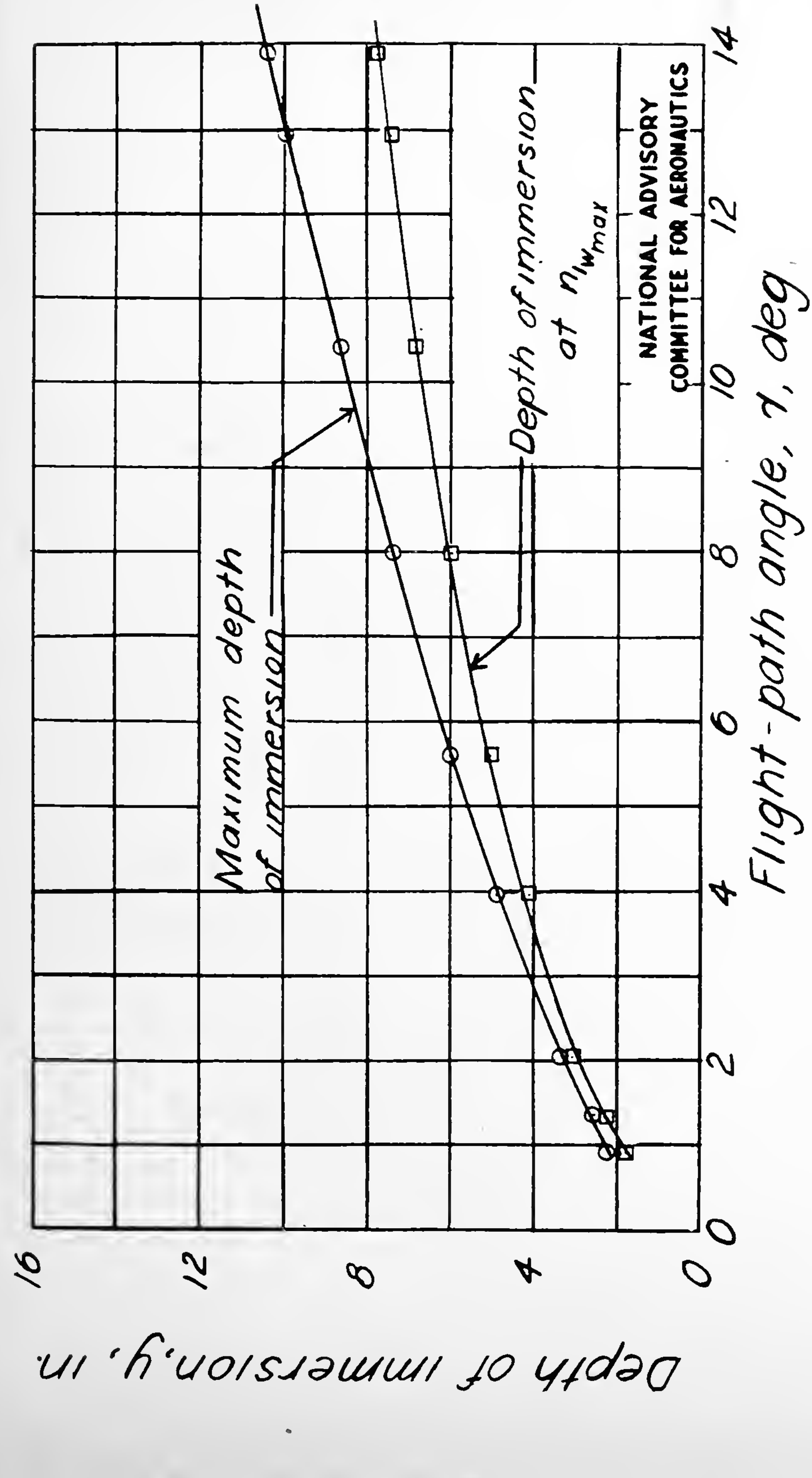

Figure 3.- Variation of maximum depth of immersion and immersion at time of maximum acceleration with flight-path angle. $\tau = 6°$; $W = 1100$ pounds.

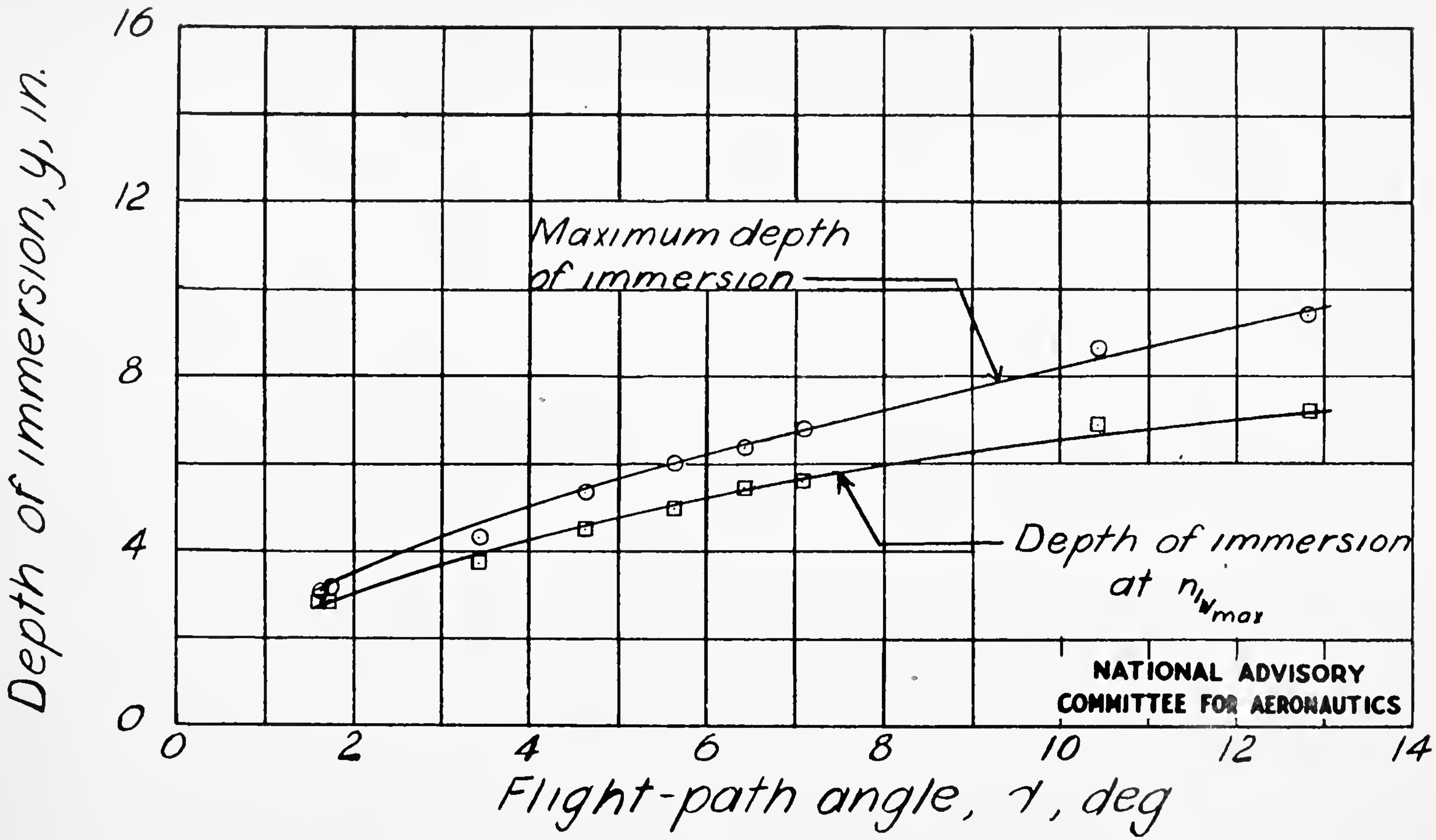

Figure 4.- Variation of maximum depth of immersion and immersion at time of maximum acceleration with flight-path angle. $\tau = 9^\circ$; $W = 1100$ pounds.